Data Fusion Approaches For WiFi Fingerprinting

Elena Simona Lohan, Jukka Talvitie
Tampere University of Technology, Tampere, Finland,
{elena-simona.lohan, jukka.talvitie}@tut.fi

Gonzalo-Seco Granados
Universitat Autonoma de Barcelona
gonzalo.seco@uab.es

***Abstract*—WiFi localization problem is basically a multi-sensor data fusion. This paper investigates the use of Bayesian and non-Bayesian Dempster Shafer (DS) data fusion in the context of WiFi-based indoor positioning via fingerprinting. Two novel DS mass choices are discussed. The positioning results are based on real-field measurement data from nine distinct multi-floor buildings in two countries. It is shown that a proper mass choice is crucial in DS processing and that, in spite of taking into account the data uncertainty, the DS data fusion is not offering significant advantage in terms of positioning performance over the Bayesian data fusion.**

Keywords—3D localization; Bayesian data fusion; Dempster Shafer (DS) theory; Received Signal Strength (RSS)

I. INTRODUCTION AND MOTIVATION

Received Signal Strength (RSS)-based indoor localization has been gaining more and more attention in the research and commercial arenas in the last few years. WiFi-based indoor positioning is one of the most promising technologies, because of three main factors: 1) WiFi-s are widely deployed in indoor scenarios, 2) a mobile device in an indoor scenario can usually hear a large number of WiFi transmitters or Access Points (APs), 3) every mobile device is able to measure the RSS from various APs in range without the need of additional hardware. Moreover, it can offer satisfactory coverage because of the typical high density of APs in various buildings of interest, and it is a preferred candidate for future mass-market global indoor localization solutions [8][11].

RSS-based fingerprinting typically consists of two stages: a training stage (done offline, either in a manual or in a crowdsourced mode) and an estimation stage [9][11]. In the training stage, RSS values from all APs in a building are collected at various grid points and they are stored in a database, forming the so-called fingerprints. The database is stored on the server of the Location Service Provider (LSP). In the estimation phase, the mobile sends its request to be positioned to the LSP server. In mobile-centric approaches, which are the focus of this paper, the mobile receives a part of the training database (e.g., corresponding to a certain area where the mobile was identified), and it makes its own measurements to the APs in its range. Based on the heard APs and on the comparison with the information stored in the database, the mobile then estimates its position. Fingerprinting is indeed one of the most widespread location solutions [6][13][14][15]. We focus on the fingerprinting methods in here, because with the advent of crowdsourced data gathering and simultaneous localization and mapping (SLAM) algorithms [18], WiFi fingerprinting is becoming more and more a realistic solution to indoor positioning.

The problem of combining the information coming from all the APs in the mobile range is basically a data fusion problem, thus the Bayesian theory is well suited and highly widespread in tackling the estimation phase of WiFi positioning [6][13]. The Bayesian data fusion is however not the only data fusion option, and several papers focusing on sensor or robotic data fusion also applied the alternative Dempster-Shafer (DS) framework in many contexts, ranging from security attack detection [16] to WiFi-based positioning [5][12].

The state-of-the-art solutions relying on stand-alone WiFi-based indoor positioning are not yet able to reach sub meter-level accuracy [3][5][12][14][15]. Additional filtering stages using past trajectory information [13] and hybrid solutions (e.g., sensors plus WiFi) [17] can increase the accuracy of stand-alone WiFi positioning, but there is still significant place to improve the stand-alone WiFi-based indoor location methods and there is need to look for alternative ways of fusing the information coming from the WiFi APs.

In addition, currently, there are not many published studies of indoor localization in multi-floor scenarios and there are very few measurements available in open source that can be used as benchmark data to test the accuracy of RSS-based algorithms. At the end of this paper, we provide also a link where parts of our measurement data, i.e. the data collected in university buildings in Tampere, are made available to the research community, in order to provide a benchmark database for indoor positioning in multi-storey buildings.

The aim in this paper is to compare the non-Bayesian DS data fusion with the Bayesian data fusion in WiFi fingerprinting. DS masses are defined in various ways based on data priors from the training stage. DS theory belongs to the category of alternative solutions to the Bayesian data fusion, and it has been very little investigated so far in the context of WiFi localization [5][12]. Previous studies [5][12] are focusing on a limited analysis of DS data fusion, with only one possible DS mass choice each. Also, the results in [5] are based on a small-scale heuristics, namely one floor only and one building. The large-scale analysis of DS data fusion with various mass choices for WiFi-based positioning is thus still missing in the current literature. Here, we introduce two novel DS mass choices, better suited to WiFi fingerprinting than previous approaches reported in the literature [5][12] and we compare the Bayesian and DS approaches based on real-field data collected from nine different multi-floor buildings in two European cities: Tampere, Finland (FIN) and Berlin, Germany (DE). We show that, the DS approach with a 2-state frame of discernment provides a slight improvement in terms of the positioning accuracy over the Bayesian combining. We also show that such accuracy improvement is also highly dependent on the mass choice, and that, with an inadequate mass choice, one can lose in the accuracy compared to Bayesian data fusion.

II. FINGERPRINTING ALGORITHMS

Fingerprinting algorithms are typically based on two stages: training off-line stage and estimation phase [8][9][10][11]. In the *training phase*, the LSP collects on a server the measurements in the buildings of interest, in the form of $(x_i, y_i, z_i, T_{i,ap})$ where x_i, y_i, z_i are the 3D coordinates of the measurement point i with respect to a local reference coordinate system, $i = 1,..., N_{grid}$, N_{grid} is the total number of measurements or grid points, and $T_{i,ap}$ is the RSS in the training phase, in logarithmic scale (dBm), coming from the ap-th AP, in the i-th grid point. Here, $ap = 1,..., N_h^{T,i}$, with $N_h^{T,i}$ being the number of heard APs in the training phase at the *i*-th point. We denote by N_{AP} the total number of APs in the building of interest (each AP means an individual MAC address, but several APs can be at the same physical location). During the measurement process, several RSS measurements are taken in the same grid point, at different time instants, and with different orientations of the mobile device. In the database, we store only an average value over all times and orientations (e.g., the mean over all the RSS values in linear scale in the same point). To reduce the size of the server database, the grid points can be saved only with a certain grid step in x and y directions. For example, a 5 m grid is an adequate trade-off between the number of stored parameters and expected positioning accuracy based on our studies. An example of the histogram of the residual RSS with respect to the mean value stored in the database is shown in Fig. 1, for a university building in Tampere. The best distribution match for the joint residuals, according to Kullback Leibler divergence criterion and 11 tested possible distributions is the Gaussian fit to the RSS residuals in dB scale (also shown in dashed lines in Fig. 1), but this is still not a perfect fit.

In the *estimation phase*, the mobile measures the RSS from all the heard APs. We denote as O_{ap} the observed RSS value (in dBm) at the mobile from the *ap*-th AP, with $ap = 1,..., N_h$, where N_h is the number of heard APs. The fingerprinting problem can be stated as: given the observations O_{ap} and the information stored in the database $(x_i, y_i, z_i, T_{i,ap})$, determine the most likely coordinate (x, y, z) of the mobile. This problem is solved by combining the evidence (or the information) coming from different APs. In order to do this, a likelihood or probability function needs to be defined for each grid point *i*. The typically used distribution in WiFi fingerprinting is the Gaussian one [8][10][11], which quantifies the probability $p_{i,ap}$ that the mobile is placed in the *i*-th grid point, being given the fact that it measured the set of values $\{O_{ap}\}_{ap=1,...,N_h}$ as:

$$p_{i,ap} = \frac{1}{\sqrt{2\pi\sigma_{ap}^2}} \exp\left(-\frac{\left(O_{ap} - T_{i,ap}\right)^2}{2\sigma_{ap}^2}\right) \qquad (1)$$

where $\sigma_{ap}{}^2 = \sigma_{ap,meas}^2 + \sigma_{ap,shad}^2$ is a noise variance that lumps together the measurement $\sigma_{ap,meas}^2$ (see Fig. 1) and shadowing errors $\sigma_{ap,shad}^2$ effects.

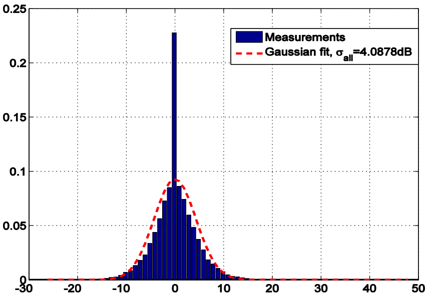

Fig. 1. Example of the distribution of RSS residuals in forming the training database. Statistics over all AP in the building.

The probability above is in fact the likelihood $p(location \mid observation)$ that the mobile is located at grid point *i*, being given the observation data from *ap*-th AP. If we apply the Bayesian rule, we can write: $p(location \mid observation) = \frac{p(observation \mid location) p(location)}{p(observation)}$, where $p(location)$ is the prior or the initial belief in the mobile location. In the absence of prior knowledge, maximizing $p(location \mid observation)$ is the same as maximizing $p_{i,ap} = p(observation \mid location)$.

In *the Bayesian linear combining* [7], the evidence from various sources is combined linearly. The probability p_i that the mobile is situated in the *i*-th grid point is:

$$p_i = \sum_{ap=1}^{N_h} p_{i,ap} = \sum_{ap=1}^{N_h} \frac{1}{\sqrt{2\pi\sigma_{ap}^2}} \exp\left(-\frac{\left(O_{ap} - T_{i,ap}\right)^2}{2\sigma_{ap}^2}\right) \qquad (2)$$

and the (x, y, z) coordinates of the mobile are estimated as those corresponding to the grid point *i* which maximizes p_i over the whole search space.

The ***search space*** is defined as a parallelepiped with edges between some minimum and maximum values in each direction (i.e., x, y, and z, respectively). The x-y minimum and maximum edges are based on the minima and maxima of the measured coordinate from the training phase in each building plus a small margin (here *-/+10* m) to account for the variations over time, mobile orientation, and presence of body losses. The z edges are based on the minimum and maximum floor heights.

In the Bayesian log-likelihood combining [2][7], the evidence is combined via the product of individual (linear) probabilities or sum of log likelihoods:

$$p_i = \prod_{ap=1}^{N_h} p_{i,ap} \Rightarrow \log p_i = \sum_{ap=1}^{N_h}\left(-\frac{1}{2}\log\left(2\pi\sigma_{ap}^{2}\right) - \frac{\left(O_{ap}-T_{i,ap}\right)^2}{2\sigma_{ap}^{2}}\right) \quad (3)$$

Again, the mobile location is taken at the grid point *i* which maximizes $\log p_i$. The log-likelihood combining is the most widely used combining method in WiFi-based positioning via fingerprinting [6][10]. The *cost function* J_i to be maximized (after the fingerprint index *i*) in the Bayesian approaches is

$$J_i = \begin{cases} p_i, \text{if linear Bayesian combining} \\ \log(p_i), \text{if log Bayesian combining} \end{cases} \quad (4)$$

The mobile estimated $\hat{\xi}$ coordinate is found in the *i*-th grid point which maximizes the cost function, or as an average of the positions of N_{nn} 'nearest neighbors', which have the N_{nn} highest values of the cost function:

$$\hat{\xi} = \frac{1}{N_{nn}} \sum_{\substack{i\in\Omega, \\ card(\Omega)=N_{nn}}} \xi_i, \quad \Omega = \{i \mid J_i \geq J_k, k \notin \Omega\} \quad (5)$$

III. Dempster-Shafer modeling with binary frame of discernment

In DS theory, the decision space is divided into mutually exclusive propositions or the so-called DS states, and all the DS states form a frame of discernment. The **frame of discernment** Θ in DS modelling consists of all hypotheses for which the information sources can provide evidence. This set Θ is finite and it consists of mutually exclusive propositions that span the hypotheses or decision space. If we denote by A_i the i-th DS state (see Section III.A for examples of choosing A_i), then $\Theta = \{A_i\}_{i=1,\dots,N}$, with *N* being the number of mutually exclusive states. If $N = 2$, then we have a binary frame of discernment. The power set is the set 2^Θ of all possible combinations within the frame of discernment, including the empty set $\varnothing$. For example, for a binary frame of discernment, the power set has 4 elements: $2^\Theta = \{A_1, A_2, \langle A_1, A_2\rangle, \varnothing\} \triangleq \{B_i\}_{i=1,\dots,4}$, for a tertiary frame of discernment, the power set has 8 elements: $2^\Theta = \{A_1, A_2, A_3, \langle A_1, A_2\rangle, \langle A_2, A_3\rangle, \langle A_1, A_3\rangle, \langle A_1, A_2, A_3\rangle, \varnothing\} \triangleq \{B_i\}_{i=1,\dots,8}$, etc. The power set basically includes evidences that support sub-sets of the frame of the discernment. Each element inside a power set is assigned a positive and sub-unitary mass $m_s(B_i) \subset [0:1]$, corresponding to the *s*-th source of evidence. These masses carry in fact the information about the degree of belief in certain evidence from the power set and they have to fulfill the following conditions:

$$\sum_{B_i \in 2^\Theta} m_s(B_i) = 1, m_s(\varnothing) = 0, 0 \leq m_s(B_i) \leq 1 \quad (6)$$

In order to combine the evidence coming from two sources and supporting a conclusion *C*, Dempster and Shafer suggested to following combination rule [1][4]:

$$m(C) \triangleq \frac{\sum_{A_i \cap A_j = C, A_i, A_j \in 2^\Theta} m_1(A_i) m_2(A_j)}{1 - \sum_{A_i \cap A_j = \varnothing, A_i, A_j \in 2^\Theta} m_1(A_i) m_2(A_j)} \quad (7)$$

where $m_1(A_i)$ is the mass associated to source 1 and supporting the conclusion A_i, $m_2(A_j)$ is the mass associated to source 2 and supporting the conclusion A_j, and A_i and A_j both support the conclusion C. For combining more than two sources of evidence, an iterative process can be used. DS theory seems therefore well suited to WiFi localization problem because it does not require prior probabilities and it allows for some 'nebulous' or uncertain states, for example $\{A_1, A_2\}$, which means that any of the states A_1 and A_2 may be true. DS theory requires that the mass functions are to be assigned in a meaningful way to various sources of evidence and this choice of the mass functions is difficult and a crucial step in DS analysis.

The DS mass choice in the context of WiFi fingerprinting is not well documented in the existing literature. In the next sub-sections, we will detail the investigated mass choices.

A. Dempster-Shafer model for WiFi-based positioning

In WiFi localization, the most straightforward approach is to divide the hypotheses space into two mutually exclusive hypotheses: either the mobile is at a certain location (***I state***) or it is not at that location (***N state***). This means that the frame of discernement is:

$$\Theta = \{I, N\} \quad (8)$$

More complex models, such as a model where each state corresponds to the mobile location at a certain floor *f*: $\Theta = \{I_f, N_f\}_{f=1,\dots N_{floors}}$ can also be envisaged, but they are out the scope of our paper. In our case, the power set becomes: $2^\Theta = \{I, N, \langle I, N\rangle, \varnothing\}$. The state $U = \langle I, N\rangle$ is the uncertain or **U state**, which tells us that we might not have sufficient evidence to decide whether the mobile is or not at a certain location.

B. Dempster-Shafer masses

If, based on the evidence coming from the *ap*-th AP, we divide first the hypotheses space into two regions: the certain region (where the mobile is either in or not in a certain grid point) and the uncertain region (where we cannot say whether the mobile is or not in a certain grid point), then we can allocate an **uncertainty factor** $u_{i.ap}$ to the mass of the uncertain U state in the *i*-th grid point. It follows that the mass of the '*certain*' state, that is the sum of I and N states, will be $1-u_{i.ap}$. The distinction between I and N states can be further done based on the probability $p_{i,ap}$ of the mobile to be at a certain grid point based on the evidence of the *ap*-th

AP (equation (1)). The $p_{i,ap}$ probability has been defined in eq. (1).

The DS masses can be thus defined as follows:

$$\begin{aligned} m_{i,ap}(I) &= (1-u_{i.ap})p_{i.ap} \\ m_{i,ap}(N) &= (1-u_{i.ap})(1-p_{i.ap}) \\ m_{i,ap}(U) &= u_{i.ap} \\ m(\varnothing) &= 0 \end{aligned} \tag{9}$$

Clearly, if $u_{i.ap}$ is chosen between 0 and 1, then the masses above are positive and less than 1, because the probabilities $p_{i.ap}$ given by (1) are sub-unitary. With the above definition, we also have that the condition (8) on masses is satisfied: $\sum_{A\subset 2^{\Theta}} m_{i,ap}(A) = m_{i,ap}(I) + m_{i,ap}(N) + m_{i,ap}(U) + m_{i,ap}(\varnothing) = 1$.

The remaining major issue is **how to choose the uncertainty factor** $u_{i.ap}$, a fact that will be discussed in Section III.C.

C. Dempster-Shafer uncertainty factor choices

The data sources of the pieces of independence (in our case the APs) can be either independent of each other or correlated with each other. In the first case, the certainty associated with a piece of evidence should be dependent only on the source of that evidence, not on other pieces of evidence. The AP evidence is likely to be a combination of correlated and uncorrelated information.

For example, some APs can transmit from exactly the same location (the cases with multiple BSSID support in WiFi), and thus the channel fluctuations experienced between the transmitter and the mobile will likely be correlated in this case. However, if the APs are distant from one another, the RSSs are likely to be uncorrelated. These assumptions about the correlated profiles when we have same positions APs and uncorrelated profiles when we have different positions APs have also been verified on the measurement data. A snapshot with the power maps of four APs, two correlated (upper part) and two uncorrelated (lower part), is shown in Fig. 2 together with the 2D correlation coefficients, namely *0.97* for the correlated case and *0.03* for the uncorrelated case. The choice of the uncertainty factor in [5] and [12] is based on the assumption that all APs are correlated between them, thus the uncertainty of one AP also depends on the evidence coming from the other APs.

In [5], the authors considered that the uncertainty has to be proportional to the fraction of the *ap*-th AP heard by the mobile, reasoning that "the stronger the RSS is, the bigger belief we give to the evidence" and interpreting the U state as the "the uncertainty about the evidence":

$$u_{i.ap}^{Zhang} = \frac{10^{\frac{O_{ap}}{10}}}{\sum_{\alpha=1}^{N_h} 10^{\frac{O_\alpha}{10}}}, ap = 1,\dots,N_h, \forall i \tag{10}$$

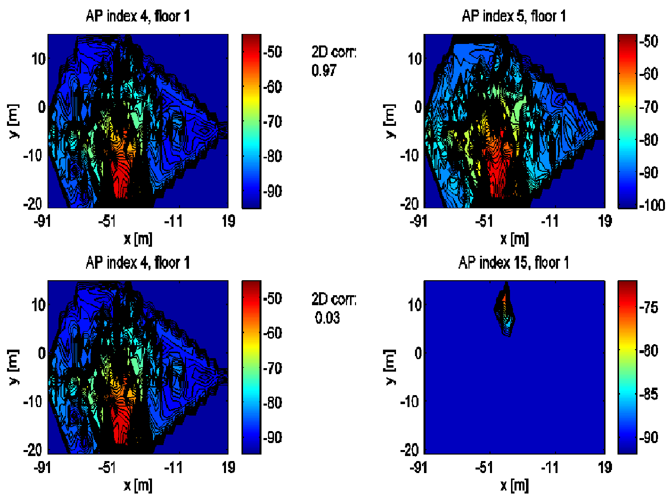

Fig. 2. Example of the RSS power maps from four access points, at one floor, in a 4-floor building. Upper plots: correlated APs (placed at the same physical location); lower plots: uncorrelated APs (APs are at different floors).

The criticism to the above choice of the uncertainty factor is that it decreases the masses associated to *I* state when RSS increases, which is counter-intuitive. In [12] the uncertainty factor was defined by associating a lower uncertainty to stronger heard APs, such that a stronger heard RSS will point out towards a higher mass for the *I* state:

$$u_{i.ap}^{var,old} = 1 - \frac{10^{\frac{O_{ap}}{10}}}{\sum_{\alpha=1}^{N_h} 10^{\frac{O_\alpha}{10}}}, ap = 1,\dots,N_h, \forall i \tag{11}$$

If intuitively we consider that all APs have initially the same credibility or trust and a lower number of heard APs should mean more uncertainty, we can also use the following mass allocation:

$$u_{i.ap}^{ct,new} = \begin{cases} 0.99, \forall ap, \forall i, \ if\ N_h = 1 \\ \frac{1}{N_h}, \forall ap, \forall i, \ if\ N_h > 1 \end{cases} \tag{12}$$

The main problems with the choice of the uncertainty factors in [5][12] (i.e., eqs. (10) and (11)) are that the masses associated to a certain source of evidence are also dependent on the evidence coming from the other sources, thus they implicitly assume that all APs are correlated. However, as illustrated in Fig. 2 and tested with the available measurement data, the power maps corresponding to APs at different locations have very low correlations between them, thus the assumption of fully correlated APs is not a valid assumption.

Moreover, the uncertainties in (10) and (11) may incorrectly give un-balanced weights to the different heard APs based on the instantaneous RSS values which are highly affected by shadowing and measurement mapping, as shown in the histograms of Fig. 1. It follows that the uncertainty factors per AP should be independent on the evidence coming from the other APs. At the same time, the uncertainty factor should be positive and sub-unitary, and it has to be defined solely based on the information arriving at the mobile from a single source, i.e., the MAC address, the instantaneous RSS from the selected AP, and, if known, the variance of the RSS residual values per AP. With this reasoning in mind and using the prior information we have from the training phase about the standard deviation σ_{ap} of the shadowing and measurement noises for each AP and about the mean residual value μ_{ap} of the mapped RSS into a single grid point, we also define the uncertainty factor of (13):

$$u_{i,ap}^{\text{var},new} = \frac{1}{\sqrt{2\pi\sigma_{ap}^2}}\exp\left(-\frac{\left(\mu_{ap}-0\right)^2}{2\sigma_{ap}^2}\right) \approx \frac{1}{\sqrt{2\pi\sigma_{ap}^2}} \quad (13)$$

As the investigations of the measurement data showed that μ_{ap} values were very small for all the buildings (of the order of *1e-6* or below), we can use the approximation of the right-hand side of (13) for the uncertainties, based only on the standard deviation of the shadowing and measurement noises.

D. Dempster-Shafer decision process

In order to find the mobile location, the cost function to be maximized in DS data fusion is equal to **the belief function** $J_i = m_i(I)$ [1] defined in (13). Each new AP will contribute to the joint masses via the following iterative process [2]: $For \quad ap = 2,...., N_h$

$$\begin{cases} J_i = m_i(I) = \dfrac{m_i(I)m_{i,ap}(I) + m_i(U)m_{i,ap}(I) + m_i(I)m_{i,ap}(U)}{1 - m_i(I)m_{i,ap}(N) - m_i(N)m_{i,ap}(I)} \\ m_i(N) = \dfrac{m_i(N)m_{i,ap}(N) + m_i(U)m_{i,ap}(N) + m_i(N)m_{i,ap}(U)}{1 - m_i(I)m_{i,ap}(N) - m_i(N)m_{i,ap}(I)}, \\ m_i(U) = \dfrac{m_i(U)m_{i,ap}(U)}{1 - m_i(I)m_{i,ap}(N) - m_i(N)m_{i,ap}(I)} \\ m_i(C) \leftarrow \dfrac{m_i(C)}{m_i(I) + m_i(N) + m_i(U)}, C \in \{I, N, U\} \end{cases} \quad (14)$$

The steps of the DS-based fingerprinting are thus:

1. Obtain the fingerprint database on the mobile from the LSP or from user measurement database.
2. Define the search space as a parallelepiped containing the whole building (see the discussion in Section2)
3. Define the probabilities based on eq. (1), with σ_{ap} equal to an estimated shadowing variance (measurement plus shadowing parts) value based on the training data, see e.g.,[3] and our examples in Fig. 1.
4. Define the uncertainty factors based on eqs. (10), (11), (12), or (13) according to the used algorithm.
5. Define the masses based on eq. (8), with uncertainty factors from Step 5.
6. Combine the evidence coming from the heard AP, according to the iterative process of eq. (14).
7. Find the position which maximizes the belief function $J_i = m_i(I)$, with $m_i(I)$ given in eq. (14) at the end of all iterations.
8. Optionally, also an average over the N_{nn} nearest neighbors. The nearest neighbors are the first N_{nn} which maximize the cost function from Step 7.

IV. MEASUREMENT-BASED RESULTS

The data gathering was done manually either with a Windows tablet (Acer Iconia Tab W500 tablet PC with Windows 7 OS) or with a Nexus tablet (Asus Nexus 7 with Android 4.3.1 OS). Both tablets included the detailed building maps, based on HERE Maps. The type of device used in each building is shown in Table 1. The field data was gathered in 9 different building in Tampere (FIN) and Berlin (DE), for three types of buildings: university (Uni), shopping centers (Center) and office buildings (Office). The position inside the building was chosen manually, based on the maps at the measured floors. We expect horizontal errors below *0.5* m in the data collection stage (and no errors in the vertical direction). The number of floors (N_f), the number of collected initially collected fingerprints (N_{fp}), the number of heard APs (N_{AP}), and the average standard deviation of measurement and shadowing errors are shown in Table IV-1.

Table IV-1. Characteristics of the measured buildings

Buil-ding	Meas. device	N_f	N_{fp}	N_{AP}[1]	Average meas. std $\sigma_{ap,meas}$ [dB]	Average shadowing std $\sigma_{ap,shad}$ [dB]
Uni 1, FIN	Windows	6	1591	309	4.08	7.39
Uni 1 (new)	Nexus	4	607	339	3.17	6.54
Uni 2, FIN	Windows	3	594	354	3.29	5.51
Center 1, FIN	Windows	3	282	69	2.47	5.41
Center 2, FIN	Windows	6	2320	326	4.13	5.49
Office 1, FIN	Nexus	7	859	995	3.49	5.21
Center 4, FIN	Nexus	4	2239	162	3.03	4.27
Office 2, DE	Nexus	10	24045	727	6.96	8.34
Center 3, DE	Nexus	4	2352	631	2.93	4.59
Center 5, DE	Nexus	7	16298	878	2.95	4.8

[1]One AP refers to one MAC address. It is possible (and very likely) that several MAC addresses are coming from the same physical location of a WiFi emitter (e.g., multiple BSSID), thus some measurements will be highly correlated between them, coming from the same physical channel. In our data analysis, we employed all the available measurements.

The measurement based results are shown in Table IV-2. The best values among all tested approaches are shown in bold-faced letters. Clearly, there are no significant differences between Bayesian and three of the DS approaches. The DS approaches with masses given in eqs. (10-12) are offering better floor detection probability than the Bayesian approaches in the majority of cases, but the average improvement is below *2%.* The newly proposed DS weights are slightly better on average than the old DS approach of [12] and much better than the old DS approach of [5]. The mass choice of [5] is clearly sub-optimal, and this case is the only one which gives consistently worse results than the others. This points out to the fact that the mass choice in DS approaches is a crucial step for a good functioning of the algorithm.

Table IV-2. Mean 3D positioning distance error [m] and the floor detection probability P_d [%].

Building	Perf. criter.	Bayesian, lin, eq. (3)	Bayesian, log, eq. (7)	Old DS masses [5]	Old DS masses [12]	New ct DS masses	New var DS masses
Uni 1, FIN	Mean pos. error [m]	5.4	6.0	20.5	8.9	**5.3**	5.4
	P_d [%]	92.45	86.73	45.92	88.36	**95.71**	**95.71**
Uni 1 (new),	Mean pos. error [m]	7.4	**7.3**	20.3	9.0	**7.3**	**7.3**

FIN	P_d [%]	93.36	92.47	55.30	90.48	95.13	**95.45**
Uni 2, FIN	Mean pos. error [m]	10.5	11.5	31.4	**9.6**	10.0	10.6
	P_d [%]	85.79	80.58	37.5	**91.48**	89.20	86.93
Center 1, FIN	Mean pos. error [m]	16.9	18.0	27.9	18.7	**16.2**	16.8
	P_d [%]	**94.88**	**94.88**	86.04	93.02	91.63	91.62
Center 2, FIN	Mean pos. error [m]	**9.8**	11.2	20.0	13.5	**9.8**	**9.8**
	P_d [%]	89.75	80.97	56.58	90.73	92.19	**92.68**
Office 1, FIN	Mean pos. error [m]	4.2	**4.0**	10.9	4.0	4.2	4.2
	P_d [%]	81.11	72.02	40.55	81.81	**86.01**	83.91
Center 4, FIN	Mean pos. error [m]	**7.3**	8.4	17.8	9.5	7.7	7.7
	P_d [%]	**87.79**	82.67	53.54	75.19	87.00	87.00
Office 2, DE	Mean pos. error [m]	**5.7**	5.8	12.6	7.4	**5.7**	**5.7**
	P_d [%]	**72.18**	64.08	33.09	62.67	71.83	71.83
Center 3, DE	Mean pos. error [m]	7.9	8.8	23.3	9.5	**7.8**	7.9
	P_d [%]	90.33	84.14	65.85	**93.94**	92.78	93.17
Center 5, DE	Mean pos. error [m]	12.1	**11.7**	22.5	12.7	12.1	12.1
	P_d [%]	**82.89**	79.39	57.85	77.29	79.43	80.07

Our analysis thus shows the following important points regarding DS analysis:

- DS analysis allows the designer to incorporate the uncertainty due to measurements and shadowing errors.
- The choice of masses in DS analysis is a crucial step and the newly proposed DS masses
- The benefit of DS approaches over Bayesian approaches, in terms of position error, is mostly seen in buildings without many open spaces between floors (e.g., typical office building).
- The floor detection probabilities of all studied approaches in Table IV-2, except the DS algorithms of [12], is very good (typically close to *85-90%*), even in the multi-floor buildings with open-spaces, such as the shopping centres.

V. Conclusions

In this paper, we have investigated the potential of DS data fusion on the context of WiFi indoor positioning via fingerprinting and we compared various data fusion approaches, based on Bayesian and non-Bayesian DS theory. The DS framework relaxes the Bayesian assumption of mutually exclusive hypotheses, allowing thus for more flexibility through the introduction of an uncertain state. We have introduced two new ways of defining the DS masses, based on variable and constant uncertainty factors and prior information collected from the training data, in order to fit with the multi-floor localization problem. The two new ways are able to take into account both cases of correlated and uncorrelated sources of evidence, but their performance gain over Bayesian approaches is still not high, pointing out towards the fact that an extra uncertainty dimension in WiFi modeling is not able to counter-balance the large shadowing and measurement variances. We have also shown that DS–based results are highly dependent on the mass function choice, and that sub-optimal mass choices may deteriorate significantly the results with respect to the Bayesian approaches. One can conclude that a DS model with binary frame of discernment is not enough to outperform the existing Bayesian approaches. On the other hand, the DS framework and mass choices presented here can offer new insights into better modeling the data quality and into quantifying the data conflict measures based on DS joint masses.

Acknowledgements

The authors express their warm thanks to the Academy of Finland (project 250266) for its financial support and to HERE for providing the measurement equipment. Parts of our measurement data for indoor localization is available at http://www.cs.tut.fi/tlt/pos/Software.htm.

References

[1] A.P. Dempster, "A generalization of Bayes inference", Journal of the Royal Statistical Society. Series B (Methodological) , pp. 205 247, 1968.

[2] C. Genest and J. Zidek, "Combining probability distributions: A critique and an annotated bibliography", Statistical Science, vol. 1, no. 1, pp. 114–148, 1986.

[3] E. Laitinen, E. S. Lohan, J. Talvitie and S. Shrestha, "Access Point Significance Measures in WiFi-based Location", in Proc. of WPNC, 2012.

[4] G.A. Shafer, Mathematical Theory of Evidence, Princeton Univ. Press, 1976.

[5] M. Zhang, S. Zhang, and J. Cao, "Fusing received signal strength from multiple access points for WiFi user location estimation", in IEEE Proc. of 2008 International conference on internet computing in science and engineering, DOI 10.1109/ICICSE.2008.24, pp. 173-180, 2008.

[6] M.M. Atia, A. Noureldin, and M.J. Korenberg, "Dynamic Online-Calibrated Radio Maps for Indoor Positioning in Wireless Local Area Networks," IEEE Transactions on Mobile Computing, vol.12, no.9, pp.1774,1787, Sept. 2013, doi: 10.1109/TMC.2012.143.

[7] N. Wanas, "Feature based architecture for decision fusion", PhD thesis University of Waterloo, 2003, http://watsup.uwaterloo.ca/pub/nwanas/thesis.pdf (active Nov 2013)

[8] R. Mautz, "Indoor positioning technologies", Habilitation thesis, ETC Zurich, Feb 2012, http://e-collection.library.ethz.ch/eserv/eth:5659/eth-5659-01.pdf (active Nov 2013).

[9] S.A. Zakavat and R.M. Buehrer (Eds), Handbook of position location: Theory, Practice and Advances, IEEE Series on Digital & Mobile Communication, Wiley-IEEE Press, ISBN 9781118184750, Nov 2011.

[10] V. Honkavirta, T. Perala, S. Ali-Loytty and R. Piche, "A Comparative Survey of WiFi Location fingerprinting Methods", in Proceedings of the 6th Workshop on Positioning, Navigation, and Communication (WPNC'09), pp.243-251, 2009.

[11] Y. Gu, A. Lo, and I. Niemegeers, "A Survey of Indoor Positioning Systems for Wireless Personal Networks", IEEE Communications Surveys & Tutorials, vol. 11, no. 1, pp.13-32, 2009.

[12] P. Kasebzadeh, G. Seco-Granados, and E.S. Lohan, "Indoor localization via WiFi path-loss models and Dempster-Shafer combining", in Proc. of IEEE ICL-GNSS conference, Jun 2014, Helsinki, Finland

[13] H. Nurminen, A. Ristimäki, S. Ali-Löytty, R. Piché, "Particle filter and smoother for indoor localization", in International Conference on Indoor Positioning and Indoor Navigation, IPIN, Oct 2013, Montbéliard-Belfort, France, pp 137-146.

[14] H. Nurminen, J. Talvitie, S. Ali-Loytty, P. Muller, E.S. Lohan, R. Piche, M. Renfors,, "Statistical path loss parameter estimation and positioning using RSS measurements in indoor wireless networks," 2012 International Conference on Indoor Positioning and Indoor Navigation (IPIN), pp.1,9, 13-15 Nov. 2012

[15] J. Yunye, S. Wee-Seng, W. Wai-Choong, "Error analysis for fingerprint-based localization," IEEE Comm. Letters, vol.14, no.5, pp.393,395, May 2010.

[16] K.G. Kyriakopoulos, F.J. Aparicio-Navarro, D.J. Parish, D.J., "Fusing multi-layer metrics for detecting security attacks in 802.11 networks," Wireless Telecomm. Symposium (WTS), 2011 , pp.1-6, Apr 2011.

[17] C. Lyu-Han, E.H.K. Wu, Ming-Hui Jin, Gen-Huey Chen, "Intelligent Fusion of Wi-Fi and Inertial Sensor-Based Positioning Systems for Indoor Pedestrian Navigation," IEEE Sensors Journal, vol.14, no.11, pp.4034-4042, Nov. 2014.

[18] S. Yang, P. Dessai, M. Verma, M. Gerla, "FreeLoc: Calibration-Free Crowdsourced Indoor Localization", in INFOCOM'13, Italy, Apr. 2013.